

Spectral modulation and squeezing at high-order neutron interferences

D. L. Jacobson and S. A. Werner

Physics Department and Research Reactor Center, University of Missouri–Columbia, Columbia, Missouri 65211

H. Rauch

Atominstytut der Österreichischen Universitäten, Schüttelstrasse 115, A-1020 Wien, Austria

(Received 1 June 1993)

A striking spectral-modulation effect has been observed by means of a proper postselection procedure under conditions where the spatial shift of the wave trains greatly exceeds the coherence length of the neutron beams traversing an interferometer. It is shown that Schrödinger-cat-like states are created by the superposition of two coherent states generated in the interferometer. These entangled states exhibit, under certain circumstances, characteristic squeezing phenomena, indicating a highly nonclassical behavior. Analogies with optical experiments are discussed.

PACS number(s): 03.65.Bz, 42.50.Dv

I. INTRODUCTION

Various postselection measurements in neutron interferometry have shown that interference fringes can be restored even in cases when the overall beam does not exhibit any interference fringes due to spatial phase shifts larger than the coherence length of the interfering beams [1–3]. The coherence length in neutron optics is defined as the inverse of the width of the momentum distribution. The loss of interference fringes at high order indicates that the simple picture which predicts interference only when wave packets spatially overlap is untrue. Interference actually occurs no matter how large the optical path difference may be. From classical optics it has been known for many years that the coherence properties manifest themselves in a spatial intensity variation for phase shifts smaller than the coherence length and in a spectral intensity variation for large phase shifts [4–9]. This phenomenon becomes more apparent for less monochromatic beams and can cause overall spectral shifts [10,11] and even squeezing phenomena [12,13].

The related phenomena for matter waves have been discussed recently [14,15] and will be elucidated in more detail in this paper. The experimental verification has been performed with a perfect crystal interferometer. Figure 1 depicts the general scheme of the measurements. Due to the rather low intensity of any neutron source, one deals with self-interference phenomena only.

II. GENERAL RELATIONS

The coherence function of stationarily overlapping wave fields is defined by the autocorrelation function of the overlapping wave functions (e.g., [16]):

$$\Gamma(\Delta) = \langle \Psi^*(0)\Psi(\Delta) \rangle, \quad (1)$$

where three-dimensional wave packets have to be considered for the description of the wave fields:

$$\Psi(\mathbf{r}) = \int a(\mathbf{k}) e^{i\mathbf{k}\cdot\mathbf{r}} d^3\mathbf{k}. \quad (2)$$

Δ represents the spatial shift of the overlapping wave functions which can be controlled by a phase shifter introduced into one of the coherent beams of the interferometer (Fig.1). Very similar to classical optics, the phase shift is given by the index of refraction n , the thickness D of the phase shifter, and the orientation of its surface $\hat{\mathbf{s}}$ relative to the direction of the incident beam $\hat{\mathbf{k}}$:

$$\Delta = \frac{(1-n)\hat{\mathbf{s}}}{(\hat{\mathbf{k}}\cdot\hat{\mathbf{s}})} \cdot D, \quad (3)$$

where n depends on the wave length λ , the coherent nucleus-neutron scattering length b_c and the particle density N of the phase shifter $n = 1 - (\lambda^2 N b_c / 2\pi)$ which gives in the most simple case a longitudinal spatial shift of $\Delta = 2\pi N b_c D / k^2$.

Standard quantum mechanics defines the momentum distribution of the beam by

$$g(\mathbf{k}) = |\Psi(\mathbf{k})|^2 = |a(\mathbf{k})|^2 \quad (4)$$

and, therefore, one gets the real part of the coherence function as the Fourier transform of the momentum distribution:

$$|\Gamma(\Delta)| \propto \left| \int g(\mathbf{k}) e^{i\mathbf{k}\cdot\Delta} d^3\mathbf{k} \right|, \quad (5)$$

which simplifies for Gaussian momentum distributions:

$$g(\mathbf{k}) \propto \exp[-(\mathbf{k} - \mathbf{k}_0)^2 / 2\delta k^2], \quad (6)$$

which characteristic widths δk_i to

$$|\Gamma(\Delta_0)| = \prod_{i=x,y,z} \exp[-(\Delta_i \delta k_i)^2 / 2]. \quad (7)$$

The mean-square distance related to $|\Gamma(\Delta)|$ defines the coherence length Δ_c^i which is for Gaussian distribution functions directly related to the minimum uncertainty relation $\Delta_c^i = 1 / (2\delta k_i)$.

The interference pattern behind the interferometer is given by the wave functions originating from beam paths I and II which are equal in amplitude and phase for the

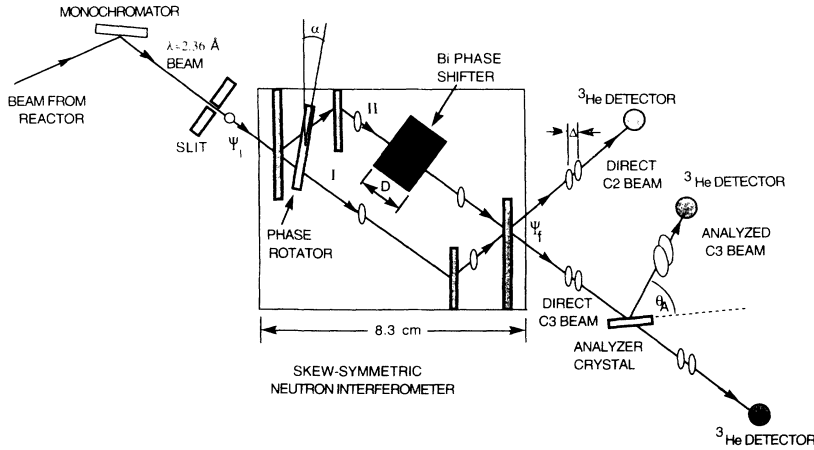


FIG. 1. Scheme of the experimental arrangement with a skew symmetrically cut perfect crystal interferometer and a postselection analyzer crystal.

forward direction (0°) and an empty interferometer because both beams are twice reflected and once transmitted ($TRR \triangleq RRT$). A phase shifter with an effective thickness $D_{\text{eff}} = D / (\hat{\mathbf{k}} \cdot \hat{\mathbf{s}})$ changes the related wave function by a phase factor

$$\exp[i(n-1)kD_{\text{eff}}] = \exp(i\Delta \cdot \mathbf{k})$$

and one gets for the individual plane wave components an intensity

$$I_0(\mathbf{r}, \mathbf{k}) = |\Psi_0^I(\mathbf{r}, \mathbf{k}) + \Psi_0^{II}(\mathbf{r} + \Delta, \mathbf{k})|^2 \propto |a(\mathbf{k})|^2 |1 + \cos[\Delta(\mathbf{k}) \cdot \mathbf{k}]|^2 \quad (8)$$

and for the overall beam

$$I_0(\Delta_0) \propto 1 + |\Gamma(\Delta_0)| \cos \Delta_0 \cdot \mathbf{k}_0, \quad (9)$$

where Δ_0 represents the spatial phase shift for the \mathbf{k}_0 component of the packet. Equation (9) describes the interference fringes when Δ_0 is varied. The formula also shows that the interference fringes disappear for spatial

phase shifts larger than the coherence lengths [$\Delta_i \geq \Delta_c^i = 1 / (2\delta k_i)$]. This behavior is shown in Fig. 2 and has been verified experimentally by several investigations for Gaussian and non-Gaussian neutron beams [17–19].

In our experiment we deal with the coherence properties along the interferometer axis (x), where the tangential components of the momentum vectors (and coherence length) do not change due to Bragg diffraction. According to basic quantum-mechanical laws, the related momentum distribution follows from Eq. (8) and for Gaussian packets it can be rewritten in the form ($k = k_x, k_y, k_z$)

$$I_0(k) \propto \exp[-(k - k_0)^2 / 2\delta k^2] \left\{ 1 + \cos \left[\chi_0 \frac{k_0}{k} \right] \right\}, \quad (10)$$

where the mean phase shift is introduced ($\chi_0 = k_0 \Delta_0 = Nb_c \lambda_0 D_{\text{eff}}$). The surprising feature is that $I_0(k)$ becomes oscillatory for large phase shifts where the

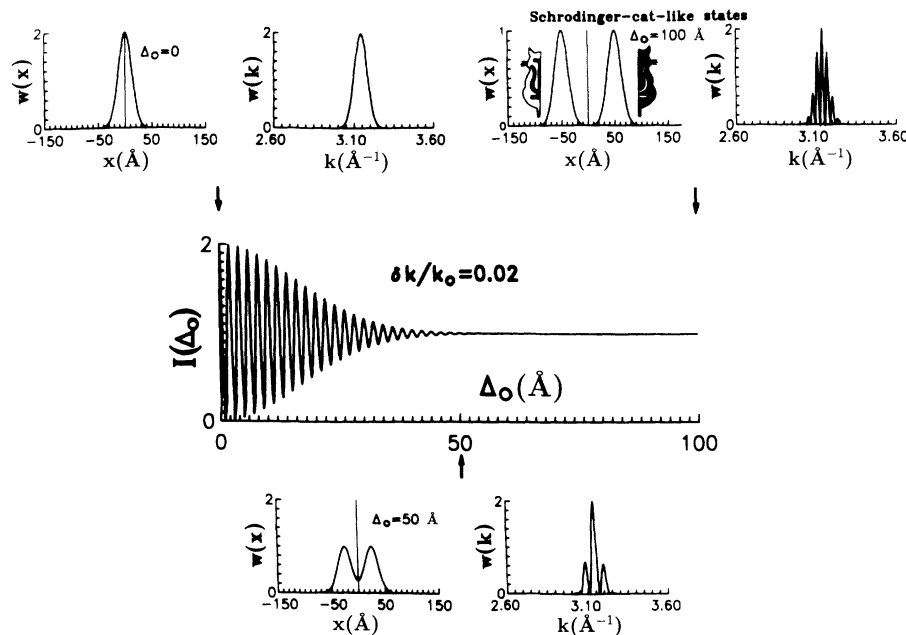


FIG. 2. Interference pattern as a function of the relative phase shift (middle) and related wave packets and momentum spectra behind the interferometer (above and below) for different values of Δ_0 (0, 50, 100 Å).

interference fringes described by Eq. (9) disappear (see Fig. 2). This indicates that interference in phase space has to be considered [20,21] rather than the simple wavefunction overlap criterion described by the coherence function [Eq. (1)]. The second beam behind the interferometer (H), just shows the complementary modulation ($I_H = I_{\text{total}} - I_0$).

The amplitude function [22] of the packets arising from beam paths I and II determines the spatial shape of the packets behind the interferometer [Eqs. (2) and (8)]:

$$I_0(x) = |\Psi(x) + \Psi(x + \Delta)|^2 \\ \propto \exp[-x^2/2\delta x^2] + \exp[-(x + \Delta_0)^2/2\delta x^2] \\ + 2 \exp[-x^2/4\delta x^2] \exp[-(x + \Delta)^2/4\delta x^2] \cos\chi_0, \quad (11)$$

which separates for large phase shifts into two peaks (Fig. 2). For Gaussian packets, δx corresponds to the coherence length Δ_c and fulfills the minimum uncertainty relation $\delta x \delta k = \frac{1}{2}$. For an appropriately large displacement ($\Delta \gg \Delta_c$), the related state can be interpreted as a superposition state of two macroscopically distinguishable states, that is, a stationary Schrödinger-cat-like state [23,24], but here first for massive particles. These states—separated in ordinary space and oscillating in momentum space—seem to be notoriously fragile and sensitive to dephasing effects [25–28]. First numerical calculations have shown that slight variations of experimental parameters (density, collimating slits, etc.) smear out the momentum distribution at large phase shifts much stronger than at low-order interferences [29]. This indicates a forced transition to a statistical mixture at high order or, equivalently, at large separations of the wave-packet parts.

III. EXPERIMENT

The experimental arrangement has been described in more detail in a previous publication [2] and it is schematically shown in Fig. 1. An additional monochromatization is applied behind the interferometer by means of various single crystals brought into Bragg position. The measurements were performed at the University of Missouri Research Reactor (MURR) with a nominal wavelength of $\lambda_0 \approx 2.36 \text{ \AA}$ and a wavelength spread of $\delta\lambda \approx 0.036 \text{ \AA}$, which is determined by the monochromator placed in front of the interferometer. The whole setup corresponds to a double-crystal arrangement between the interferometer crystal (mosaic spread $\eta_i \rightarrow 0$, Bragg angle Θ_i) and the additional analyzer crystal (mosaic spread η , Bragg angle Θ_A). For Gaussian-shaped beams and crystal reflectivities, the momentum distribution behind the analyzer becomes changed according to (e.g., [30])

$$\left| \frac{\delta k'}{\delta k} \right|^2 \simeq \frac{(\delta k_A^2)}{(\delta k)^2 + (\delta k_A)^2}, \quad (12)$$

with

$$\left(\frac{\delta k_A}{k_0} \right)^2 \simeq \eta^2 \left| \frac{\cos\Theta_i \cos\Theta_A}{\sin(\Theta_i \pm \Theta_A)} \right|^2,$$

where the positive sign corresponds to the parallel setting and the negative sign to the antiparallel configuration.

Measurements of the wavelength spectrum were made with a narrow mosaic silicon crystal which reflects in the parallel position a very narrow band of neutrons only ($\delta k'/\delta k \approx 0.05$) causing an enhanced visibility at large phase shifts (Fig. 3). The related coherence function which corresponds to the amplitude (contrast) of the interference pattern is shown in Fig. 4 [2]. This feature shows that an interference pattern can be restored even behind the interferometer by means of a proper postselection procedure. In this case the overall beam does not show interference fringes anymore and the wave packets originating from the two different beam paths do not overlap.

The momentum distribution has been measured by scanning the analyzer crystal through the Bragg position. The related results are shown in Fig. 5 for different phase shifts. These results clearly demonstrate that the predicted spectral modulation [Eq. (10)] appears when the interference fringes of the overall beam disappear. The modulation is somehow smeared out due to averaging processes across the beam due to various imperfections, unavoidably existing in any experimental arrangement. The contrast of the empty interferometer was 60%.

IV. DISCUSSION

The results clearly demonstrate that a spectral modulation can be observed in neutron interference experiments at high interference order and that interference has to be treated in phase space rather than in ordinary space. It seems that the plane-wave components of the wave pack-

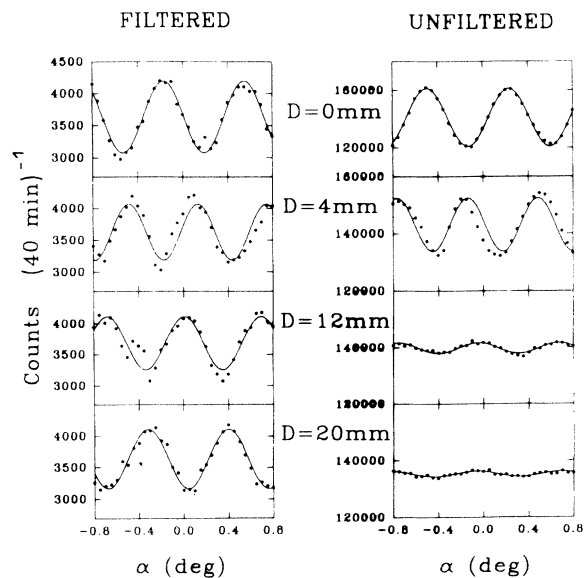


FIG. 3. Interference pattern of the overall beam ($\delta k/k_0 = 0.012$) and the beam reflected from a nearly perfect crystal analyzer in the antiparallel position ($\delta k'/k_0 = 0.0003$).

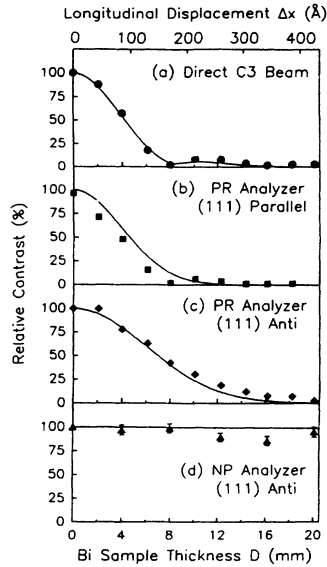


FIG. 4. Coherence function measured from the visibility of the interference pattern for different degrees of postselection of momentum states: (a) direct beam measured without analyzer, (b) pressed silicon analyzer, and (c) nearly perfect silicon analyzer (see Fig. 3).

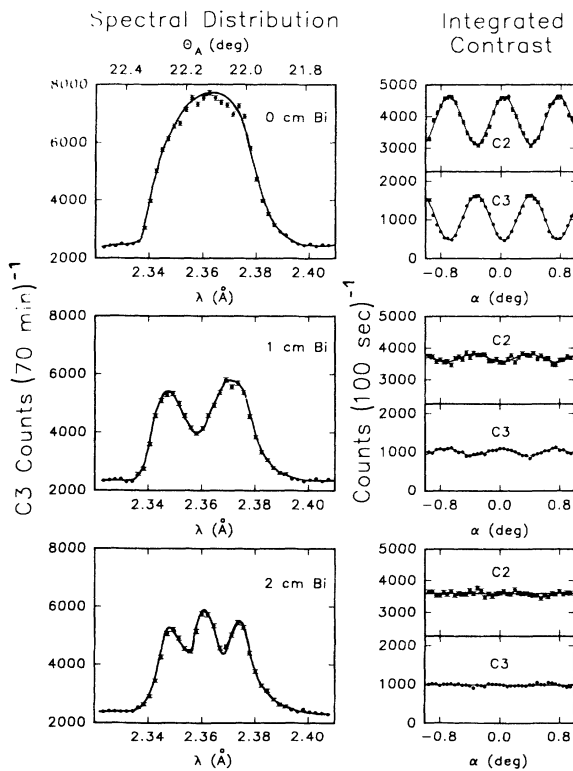


FIG. 5. Measured spectral modulation of the outgoing beam and the residual interference pattern for different bismuth phase-shifter thicknesses. The wavelength resolution of the analyzer was 0.002 \AA . The integrated contrast is shown for the deviated and for the forward beam; the spectral distribution measurements relate to the forward beam only.

ets, i.e., narrow-bandwidth components, interact over a much larger distance than the size of the packets. This interaction guides neutrons of certain momentum bands to the 0° or H beam, respectively. These phenomena throw a new light on the discussion of Schrödinger-cat-like situations in quantum mechanics and, therefore, on the discussion about Einstein-Podolsky-Rosen (EPR) experiments too [14,31–33]. Spatially separated packets remain entangled in phase space and nonlocality appears as a result of this entanglement. The analogy with optical experiments performed in the time-frequency domain is striking [8]. An analog situation exists in neutron spin-echo systems where multiple spin rotation plays a role equivalent to that of high-order interferences as discussed here [34].

Each peak in the momentum distribution corresponds to a different number of phase shifts experienced by the neutrons of that wavelength band during its passage through the interferometer. In that sense, the minimum quantum unity of the incident wave packet becomes a new quantity representing different quantum states with distinguishable properties. This kind of labeling shows that constructive interference is restricted to that wavelength band only—a situation similar to that where new states have been created due to lattice diffraction inside the interferometer [35].

The new quantum states created behind the interferometer can be analyzed with regard to their uncertainty properties. Analogies between a coherent-state behavior and a free but coherently coupled particle motion inside the interferometer have been addressed previously [36]. In such cases, the dynamical conjugate variables x and p minimize the uncertainty product with identical uncertainties $(\Delta x)^2 = (\Delta k)^2 = \frac{1}{2}$ (in dimensionless units). Using $I_0(k)$ and $I_0(x)$ [Eqs. (10) and (11)] as distribution functions we get in our case

$$\begin{aligned} \langle (\Delta x)^2 \rangle &= \langle x^2 \rangle - \langle x \rangle^2 \\ &= (\delta x)^2 \left[1 + \frac{(\Delta_0/2\delta x)^2}{1 + e^{-\Delta_0/2\delta x})^2/2} \cos(\Delta_0 k_0) \right] \end{aligned} \quad (13)$$

and (for $\delta k/k_0 \ll 1$)

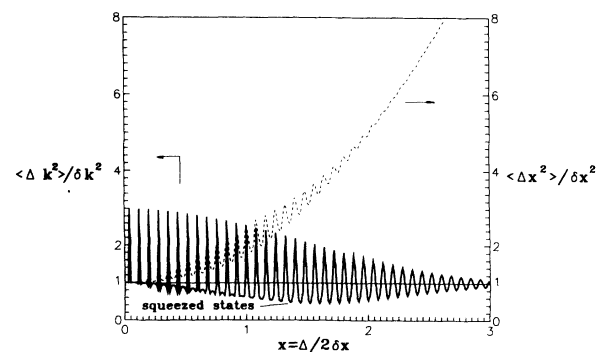


FIG. 6. Spatial and momentum uncertainties of the outgoing beams with the indication of squeezing in the momentum domain.

$$\langle (\Delta k)^2 \rangle = \langle k^2 \rangle - \langle k \rangle^2 = (\delta k)^2 \left\{ 1 - \left[\frac{\Delta_0}{2\delta x} \right]^2 \frac{e^{-(\Delta_0/2\delta x)^2/2} \cos(\Delta_0 k_0) + e^{-(\Delta_0/2\delta x)^2}}{\left[1 + e^{-(\Delta_0/2\delta x)^2/2} \cos(\Delta_0 k_0) \right]^2} \right\}. \quad (14)$$

These relations are shown in Fig. 6, indicating that for $(\Delta k)^2$ a value below the coherent-state value can be achieved, which in quantum optic terminology means squeezing [12,37,38]. One emphasizes that a single coherent state does not exhibit squeezing, but a state created by superposition of two coherent states can exhibit a considerable amount of squeezing. Thus, highly nonclassical states can be made by the power of the quantum-mechanical superposition principle.

ACKNOWLEDGMENTS

This work was supported by the Physics Division of NSF (Grant No. PHY-9024608) and the Austrian Science Foundation FWF (Project No. P8456). Valuable help in carrying out analytical and numerical calculations was given by Yongde Zhang (Hefei and Wien) and Martin Suda (Seibersdorf), and technical assistance by Helmut Kaiser (Columbia).

-
- [1] S. A. Werner, R. Clothier, H. Kaiser, H. Rauch, and H. Wölwitsch, *Phys. Rev. Lett.* **67**, 683 (1991).
 - [2] H. Kaiser, R. Clothier, S. A. Werner, H. Rauch, and H. Wölwitsch, *Phys. Rev. A* **45**, 31 (1992).
 - [3] H. Rauch, H. Wölwitsch, R. Clothier, H. Kaiser, and S. A. Werner, *Phys. Rev. A* **46**, 49 (1992).
 - [4] L. Mandel, *J. Opt. Soc. Am.* **52**, 1335 (1962).
 - [5] L. Mandel and E. Wolf, *Rev. Mod. Phys.* **37**, 231 (1965).
 - [6] F. Heineger, A. Herden, and T. Tschudi, *Opt. Commun.* **48**, 237 (1983).
 - [7] D. F. V. James and E. Wolf, *Phys. Lett. A* **157**, 6 (1991).
 - [8] X. Y. Zou, T. P. Grayson, and L. Mandel, *Phys. Rev. Lett.* **69**, 3041 (1983).
 - [9] G. S. Agarwal and D. F. V. James, *J. Mod. Opt.* **40**, 1431 (1993).
 - [10] E. Wolf, *Phys. Rev. Lett.* **63**, 2220 (1989).
 - [11] D. Faktis and G. M. Morris, *Opt. Lett.* **13**, 4 (1988).
 - [12] W. Schleich, M. Pernigo, and Fam Le Kien, *Phys. Rev. A* **44**, 2172 (1991).
 - [13] J. Janski and A. V. Vinogradov, *Phys. Rev. Lett.* **64**, 2771 (1990).
 - [14] H. Rauch, *Phys. Lett. A* **173**, 240 (1993).
 - [15] H. Rauch, *Proceedings in Quantum Measurement and Control*, edited by E. Ezawa and Y. Murayama (North-Holland, Amsterdam, 1993) p. 223.
 - [16] M. Born and E. Wolf, *Principles of Optics* (Pergamon, New York, 1975).
 - [17] H. Rauch, in *Neutron Interferometry*, edited by U. Bonse and H. Rauch (Clarendon, Oxford, 1979), p. 161.
 - [18] H. Kaiser, S. A. Werner, and E. A. George, *Phys. Rev. Lett.* **50**, 563 (1983).
 - [19] R. Clothier, H. Kaiser, S. A. Werner, H. Rauch, and H. Wölwitsch, *Phys. Rev. A* **44**, 5357 (1991).
 - [20] W. Schleich and J. A. Wheeler, *Nature* **326**, 574 (1987).
 - [21] W. Schleich, D. F. Walls, and J. A. Wheeler, *Phys. Rev. A* **38**, 1177 (1988).
 - [22] J.-M. Levy-Leblond and F. Balibar, *Quantics* (North-Holland, Amsterdam, 1990).
 - [23] A. Legett, *Proceedings, Foundations of Quantum Mechanics in the Light of New Technologies*, edited by S. Kamefuchi (Physical Society of Japan, Tokyo, 1984), p. 74.
 - [24] B. Yurke, W. Schleich, and D. F. Walls, *Phys. Rev. A* **42**, 1703 (1990).
 - [25] D. F. Walls and G. J. Milburn, *Phys. Rev. A* **31**, 2403 (1985).
 - [26] R. J. Glauber, *Ann. N. Y. Acad. Sci.* **480**, 336 (1986).
 - [27] M. Namiki and S. Pascazio, *Phys. Rev. A* **44**, 39 (1991).
 - [28] H. Zurek, *Phys. Today*, **44** (10), 36 (1991).
 - [29] H. Rauch and M. Suda (unpublished).
 - [30] G. Cagliotti and D. Tocchetti, *Nucl. Instrum. Methods* **32**, 181 (1965).
 - [31] A. Einstein, B. Podolsky, and N. Rosen, *Phys. Rev.* **47**, 777 (1935).
 - [32] D. M. Greenberger, M. A. Horne, and A. Zeilinger, in *Bell's Theorem: Quantum Theory and Conceptions of the Universe*, edited by M. Kafatos (Kluwer, Dordrecht, 1989), p. 69.
 - [33] N. D. Mermin, *Phys. Rev. Lett.* **65**, 1838 (1990).
 - [34] G. Badurek, H. Weinfurter, R. Gähler, A. Kollmar, S. Wehinger, and A. Zeilinger, *Phys. Rev. Lett.* **71**, 307 (1993).
 - [35] H. Rauch and J. Summhammer, *Phys. Rev. A* **46**, 7284 (1992).
 - [36] H. Rauch, J. Summhammer, M. Zawisky, and E. Jericha, *Phys. Rev. A* **42**, 3726 (1990).
 - [37] D. F. Walls, *Nature* **306**, 141 (1983).
 - [38] S. L. Braunstein and R. I. McLachlan, *Phys. Rev. A* **35**, 1659 (1987).

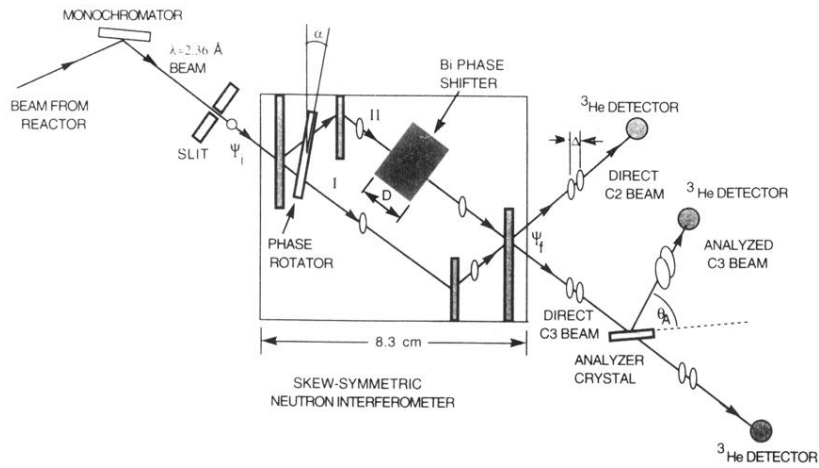


FIG. 1. Scheme of the experimental arrangement with a skew symmetrically cut perfect crystal interferometer and a postselection analyzer crystal.